Assessment of the long term behaviour of structural adhesives in the context of NSM flexural strengthening technique with prestressed CFRP laminates

I. G. Costa[1], J. A. O. Barros[2]
[1] University of Minho, DEC - Azurém 4800-058 Guimarães, Portugal, ines.costa@civil.uminho.pt
[2] University of Minho, DEC - Azurém 4800-058 Guimarães, Portugal, barros@civil.uminho.pt

Keywords: Analytical analysis; Long-term tests; Epoxy.

SUMMARY
This study is part of a research project that aims to develop a new strategy to apply prestressed Carbon Fibre Reinforced Polymer (CFRP) laminates according to the Near Surface Mounted (NSM) technique for the flexural strengthening of Reinforced Concrete (RC) elements. This paper includes a state-of-the-art covering the following main aspects: (1) theoretical models used to predict creep behaviour; (2) standards proposing experimental setups and test procedures for the evaluation of creep in adhesives (3) reliable analytical models, which predictive performance has been assessed from experimental creep tests. The paper also includes an experimental program that was carried out to assess the creep model that best describes the bi-component adhesive selected to be used with the NSM technique in development. The main results are here presented and discussed.

1. INTRODUCTION

Prestressing FRPs is known to be a strategy that improves the efficacy of FRP reinforcement since the width of existing cracks can be reduced or completely closed and the appearance of new fissures can be delayed, which results in benefits in terms of structural integrity and concrete durability [1-3]. Furthermore, the load carrying capacity of RC elements for service limit states increases with the prestress level applied to the FRP reinforcement. However, as in the case of common prestressed reinforcement steel, it is necessary to quantify the prestress losses associated with this technology, mainly with regard to the time-dependent losses, which result essentially from the creep/shrinkage of the substrate and the relaxation of the prestressing material.

While the FRP reveals low prestress losses, as a result of their relatively low elastic modulus [4], and low stress relaxation [5], excessive creep/shrinkage of the substrate may cause significant losses of prestress in the FRP. In spite of epoxy adhesives being capable of presenting a certain amount of shrinkage during the curing process, this shrinkage stops when complete cure is achieved [6-7] and creep becomes the most relevant phenomenon.

The most important function of the structural adhesive is to transmit stress appropriately over large areas without loss of integrity [8]. A careful bibliographic review was carried out to better understand how epoxy adhesives are expected to behave over time, and revealed that the level of applied stress and the environmental exposure conditions [8], mostly temperature and humidity, are the factors that most affect the long-term performance of the adhesive. In that paper it was verified that most of the analytical equations presented are based on rheological models, with occasional minor adjustments, and they describe with adequate accuracy the behaviour of the epoxy adhesive under sustained load. The creep behaviour of plastic materials can severely influence the global performance of a prestressed FRP-NSM system and therefore, the determination of this creep performance is sometimes

as essential as the assessment of common tensile properties as tensile strength and elastic modulus. Given the possibility of creep behaviour being relevant for purposes of material characterization, ASTM and ISO [9-10], normalized the execution of these creep experimental tests.

2. RHEOLOGICAL MODELS

Structural epoxy adhesives exhibit significant viscoelastic behaviour, since their deformation under constant stress varies considerably in time, which can compromise the capacity of stress transmission from the FRP to the substrate. This viscoelastic behaviour is typically modelled using rheological models that is usually demonstrated by means of Hookean springs (Figure 1a) and Newtonian dashpots (Figure 1b) that replicate, respectively, the elastic and viscous components of the material's behaviour [11].

There are essentially three classical rheological models, all named after their proposers: Maxwell, Kelvin and Burgers. The last of these models is the result of the assemblage of the previous two, as depicted in Figure 2a. Therefore, the strain response of Burgers (Figure 2b) model is the addition of the strain responses produced by Maxwell and Kelvin models, and can be expressed in mathematical terms by Eq. (1).

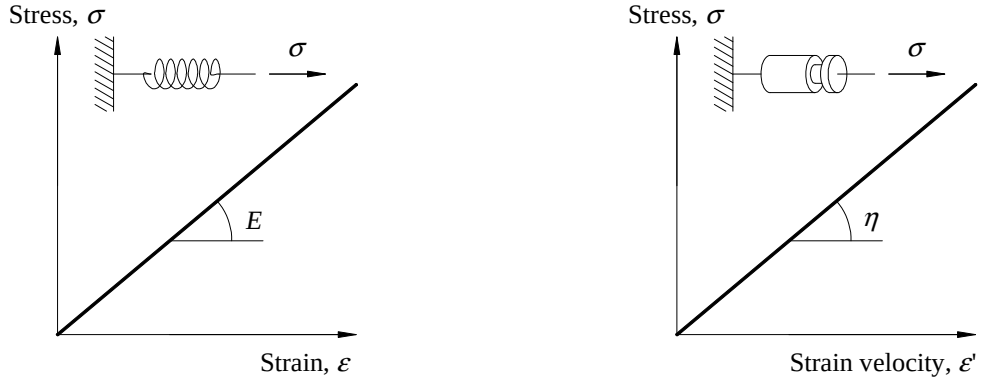

(a) (b)

Figure 1: Diagram of (a) linear elastic behaviour and (b) linear viscous behaviour.

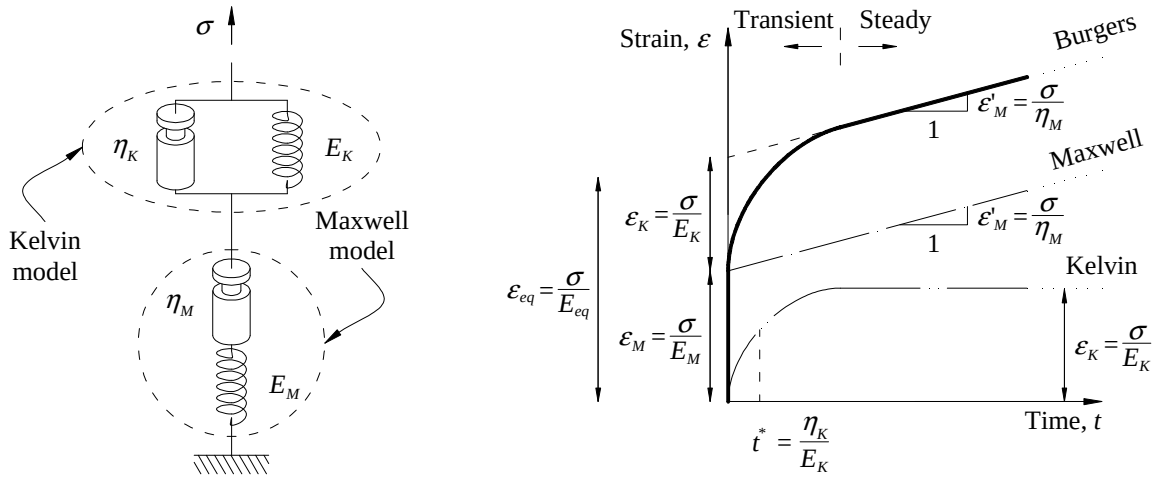

(a) (b)

Figure 2: Rheological models: (a) Burgers model schematization and (b) Strain response of different rheological models.

$$\varepsilon(t) = \underbrace{\frac{\sigma}{E_M} + \frac{\sigma}{\eta_M}t}_{\text{Maxwell response}} + \underbrace{\frac{\sigma}{E_K}\left(1 - e^{-\frac{E_K}{\eta_K}t}\right)}_{\text{Kelvin response}} \quad (1)$$

3. EXPERIMENTAL PROGRAM

With the purpose of verifying the applicability of these rheological models to describe the creep behaviour of the structural adhesive to be used in prestressed FRP applications, an experimental program was carried out. The recommendations of the applicable standards [9-10] were combined to meet, as much as possible, all their requirements. In brief, both standards recommend that load is applied smoothly to a standard dumbbell epoxy specimen within 1 to 5 seconds and maintained for at least 1000 hours (approximately 42 days). These tests need be repeated for an appropriate number of stress levels, for each applicable combination of temperature/humidity. In this experimental program three levels of stress were applied to each of the three series that were tested under a constant temperature of 20ºC and constant relative humidity of 60%.

3.1 Tensile Properties

Preliminary tensile tests, performed according to ISO 527-2 [12], revealed that the adhesive selected, at 3 days of age, achieves a stable elasticity modulus as well the maximum tensile strength (around 20 MPa), and is therefore considered as completely cured at that age. Nevertheless, in both series executed, the typical tensile properties were assessed at the loading age (herein identified as t = 0 hours, which corresponds to an adhesive with 3 days of age), and in the end of the creep tests (1000 hours), as reported in Table 1. It was noted that the elasticity modulus ($E_{0.5\sim2.5‰}$) of the specimens from all series was practically maintained from 0 h to 1000 h, although the coefficient of variation in series III was unusually high. Regarding the tensile strength evolution, $f_{max,t=0\ h}$, series I and II exhibited the expected value, 20 MPa, while series III only presented 75% of the estimated strength.

Table 1: Tensile properties of the adhesive.

Series	***t = 0 hours***		***t = 1000 hours***	
	$E_{0.5\sim2.5‰}$	f_{max}	$E_{0.5\sim2.5‰}$	f_{max}
Series I	7.70 GPa (0.16 GPa) [2%]	20.2 MPa (2.2 MPa) [11%]	7.61 GPa (0.29 GPa) [4%]	20.9 MPa (1.3 MPa) [6%]
Series II	6.79 GPa (0.41 GPa) [6%]	20.3 MPa (1.7 MPa) [8%]	6.36 GPa (0.29 GPa) [5%]	17.7 MPa (1.6 MPa) [9%]
Series III	6.72 GPa (0.74 GPa) [11%]	15.0 MPa (2.5 MPa) [16%]	7.36 GPa (0.84 GPa) [11%]	15.7 MPa (5.4 MPa) [35%]

Average, (Standard Deviation) and [Coefficient of variation]

3.2 Experimental tensile creep curves

The used creep specimens presented the same geometry adopted for tensile tests, and defined by ISO 527-2. In each series, three stress levels were applied to the standard specimens in a creep table prepared to amplify 3 times a given static load, which permitted applying approximately 4, 8 and 12 MPa in each specimen (Figure 3a). However, as load was applied by means of standard weights, the real stress level generated was also influenced by the specimen's cross section area, A, which was difficult to maintain rigorously the same in all the specimens. The specimens were instrumented with

two strain-gauges, type BFLA-2-3-3L, from TML Strain Gauges with a 2 mm measuring length installed precisely at the centre of each face (Figure 3b).

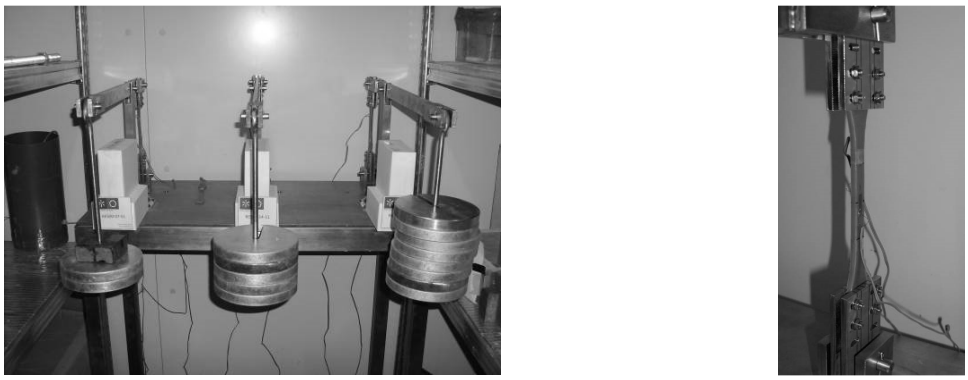

(a) (b)

Figure 3: Experimental setup: (a) creep table and (b) aspect of an instrumented specimen.

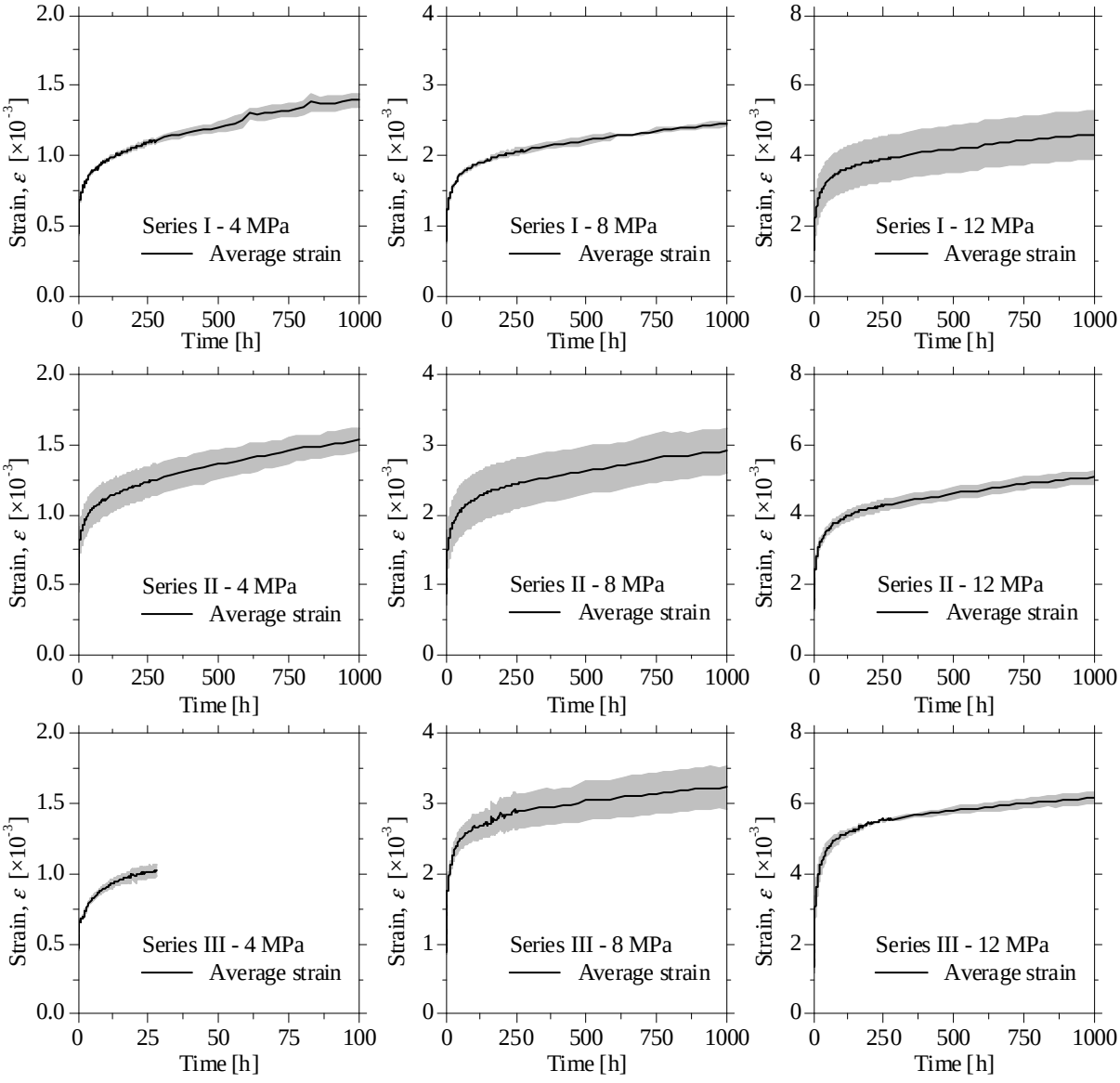

Figure 4: Experimental tensile creep range and experimental curves.

The tests performed suggest that the material characteristics distribution is not perfectly uniform since opposite strain-gauges presented in some cases very different levels of strain (Figure 4). For that reason the determination of the parameters of the curves was performed using the average value of strains measured in each specimen. Observing the information given in Figure 2b and the obtained experimental results, Burgers model seems to be the most suitable to describe the material's behaviour.

3.3 Curve Parameters

From the average strain curves, the following values were assessed as follows:
- ε_M, the instantaneous strain mobilized, corresponding to the strain at the instant $t = 0$;
- ε'_M, the long-term strain velocity, which was fixed to be the average slope from t = 666.7~1000 h;
- ε_{eq}, the equivalent initial strain that results from the interception of ε'_M branch and the strain ordinate axis;
- t^* is the retardation time that is, by definition, the time necessary to achieve approximately 63% of Kelvin's maximum strain.

The values obtained by this method are presented in Table 2. However, the determination of the retardation time, t^*, involves the deconstruction of the experimental curve using the parameters previously obtained and according to Eq. (2). The result correspondent to this deconstruction is depicted in Figure 5. The rheological parameters necessary to determine Eq. (1) can be easily obtained by performing basic calculations, as reported in Figure 2b, and are presented in Table 3.

$$\%\varepsilon_K = \frac{E_K}{\sigma}\varepsilon(t) - \frac{E_K}{E_M} - \frac{E_K t}{\eta_M} \tag{2}$$

Table 2: Notable tensile creep points.

Series	σ [MPa]	A [mm^2]	ε_M [×10^{-3}]	ε'_M [×10^{-3}/h]	ε_{eq} [×10^{-3}]	t^* [h]
Series I	4.3	43.486	0.4452	4.0987E-04	1.0107	26
	7.8	43.278	0.7890	4.9927E-04	1.9688	25
	11.9	43.067	1.2822	8.8907E-04	3.7497	22
Series II	4.6	41.272	0.5108	3.7700E-04	1.1676	20
	8.0	42.494	0.8877	6.1171E-04	2.3208	20
	11.3	45.296	1.3036	1.0351E-03	4.0796	20
Series III	4.5	42.003	0.4658	-	-	-
	8.1	41.763	0.8976	3.9384E-04	2.8503	19
	11.8	43.487	1.3626	6.6730E-04	5.4986	19

Table 3: Rheological parameters.

Series	σ [MPa]	E_M [GPa]	η_M [GPa·h]	E_K [GPa]	η_K [GPa·h]	n
Series I	4.3	9.48	11890	7.92	202	0.48
	7.8	9.90	15640	6.62	164	0.48
	11.9	9.31	13425	4.84	105	0.45
Series II	4.6	8.06	13582	6.30	109	0.57
	8.0	8.96	13001	5.55	109	0.52
	11.3	8.71	10964	4.09	81	0.49
Series III	4.5	9.78	-	-	-	-
	8.1	9.02	20547	4.14	77	0.53
	11.8	8.67	17714	2.86	54	0.48

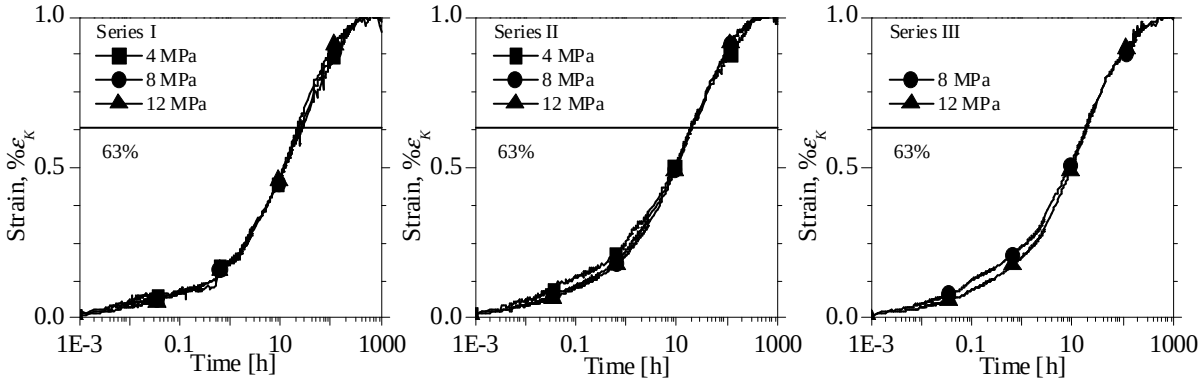

Figure 5: Percentage of Kelvin's maximum strain vs. time (time in logarithmic scale).

Performing a direct substitution of the rheological parameters in Eq. (1), the strain prediction is not as precise as expected (see Figure 6). Due to this fact, Burgers equation was slightly modified, according to bibliographic research findings [8]. Feng *et al.* [8] explained in their work that the presence of moisture can assist molecular mobility and, therefore, decrease the amount of energy required to deform the material. In consequence, the original form of Burgers model was adapted, resulting Eq. (3). The parameter *n* was therefore included in the analytical formulation and estimated to minimize the difference between analytical and experimental curve, producing a much more accurate projection, as depicted in Figure 7.

$$\varepsilon(t) = \frac{\sigma}{E_M} + \frac{\sigma}{\eta_M} t + \frac{\sigma}{E_K}\left(1 - e^{-\left(\frac{E_K}{\eta_K} t\right)^{1-n}}\right) \tag{3}$$

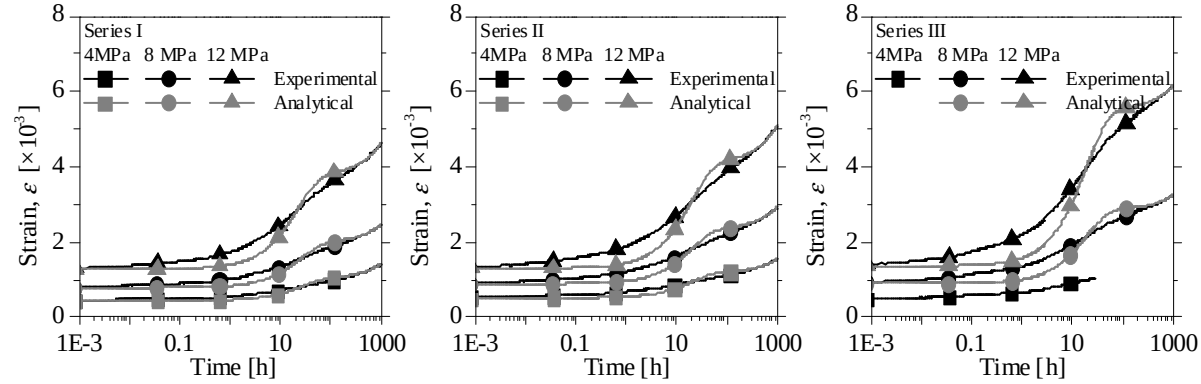

Figure 6: Analytical curves obtained by direct substitution (time in logarithmic scale).

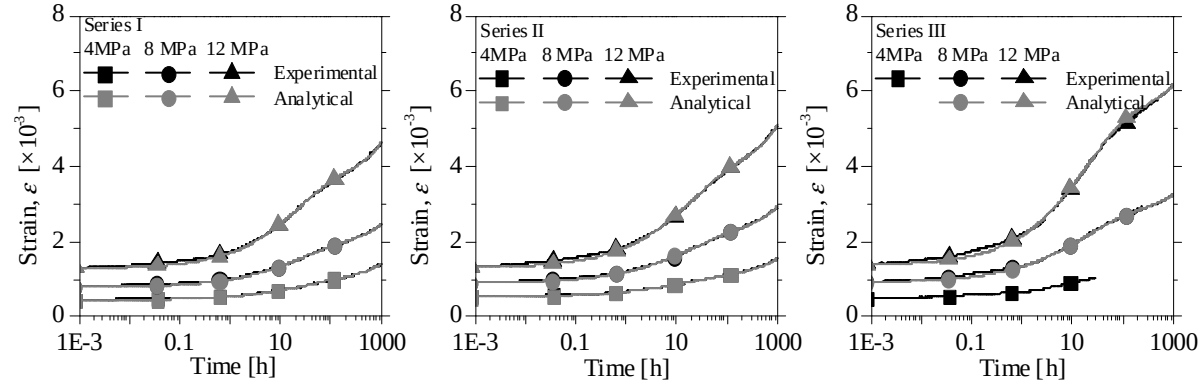

Figure 7: Analytical curves obtained by including the parameter *n* (time in logarithmic scale).

3.4 Analysis of the parameters defining the tensile creep curves

Examining the obtained parameters it was noticed that in all series the rheological elements present predominantly linear tendency, which suggests that this material exhibits linear elastic and viscous behaviour.

It was verified that the elasticity modulus obtained in the control tensile tests (Table 1) is 20% lower than the one obtained in the experimental creep tests (Figure 8), which is expectable, considering that the loading process was relatively rapid. Still, the values of the elastic modulus between series were compatible with the control tensile tests, confirming that it decreased from series I to III.

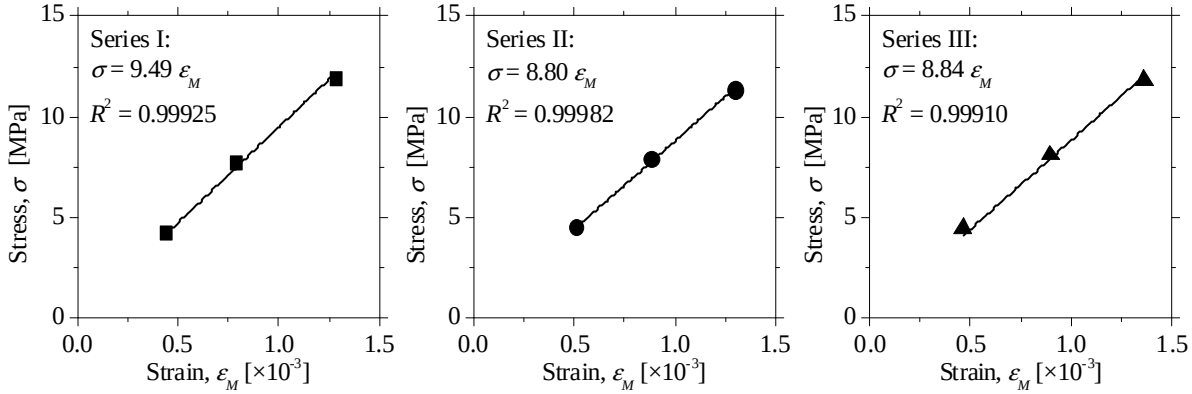

Figure 8: Applied stress vs. initial strain relationship.

Concerning Kelvin's strain, defined by $\varepsilon_K = \varepsilon_{eq} - \varepsilon_M$, the linear regression fitting also presented a good adjusted r-square value (Figure 9). Additionally, the values obtained for the equivalent long-term Kelvin's modulus, E_K, exhibited the same decreasing trend in all series, suggesting that these quantities may somehow be related, although this investigation is not sufficient to conclude about this matter.

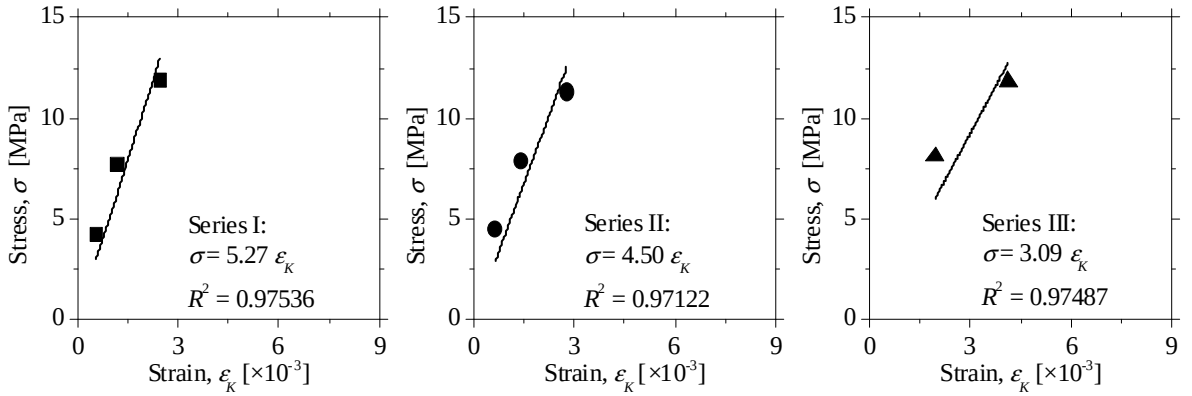

Figure 9: Stress vs. Kelvin's strain relationship.

Analysing the viscous components, it was noticed that although the linear regression showed relatively good performance, it is possible that some of these parameters are less constant. The decrease of slope between consecutive points visible in Figure 10 when determining Maxwell dashpot coefficient (Figure 10) supports this fact. Additionally it is not uncommon that with the proximity of the material's ultimate resistance parameters are more prone to decline.

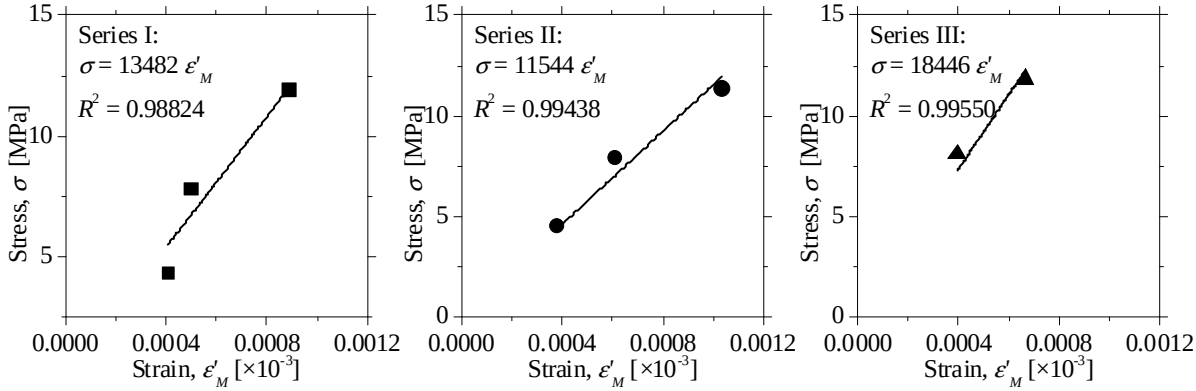

Figure 10: Stress vs. strain velocity relationship.

Regarding Kelvin's dashpot, defined by η_K, is not possible to construct the elementary stress vs. strain velocity plot since the strain velocity is continually varying in the first ages *i.e.*, the derivative of the strain is not constant as in the case of Maxwell's dashpot. However, plotting the retardation time over the stress, it can be observed that this value is in most cases practically constant (Figure 11). Since by definition the retardation time is $t^* = \eta_K / E_K$, and is constant in this experimental program, and the obtained results demonstrated that E_K is also constant, η_K is necessarily constant.

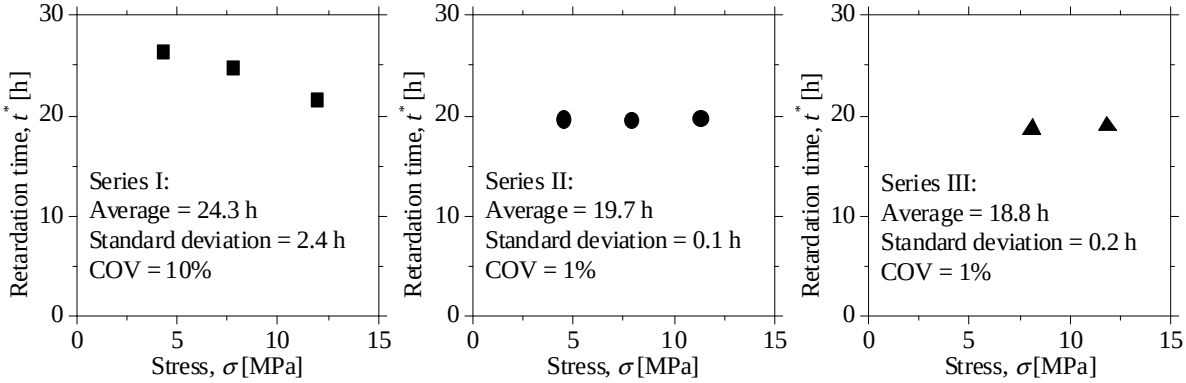

Figure 11: Retardation time vs. stress relationship.

Figure 12 represents the values of the *n* parameter of Eq. (3). Taking into account the average values and the corresponding COV, it can be concluded that a global average value could reasonably represent of the behaviour of the tested adhesive.

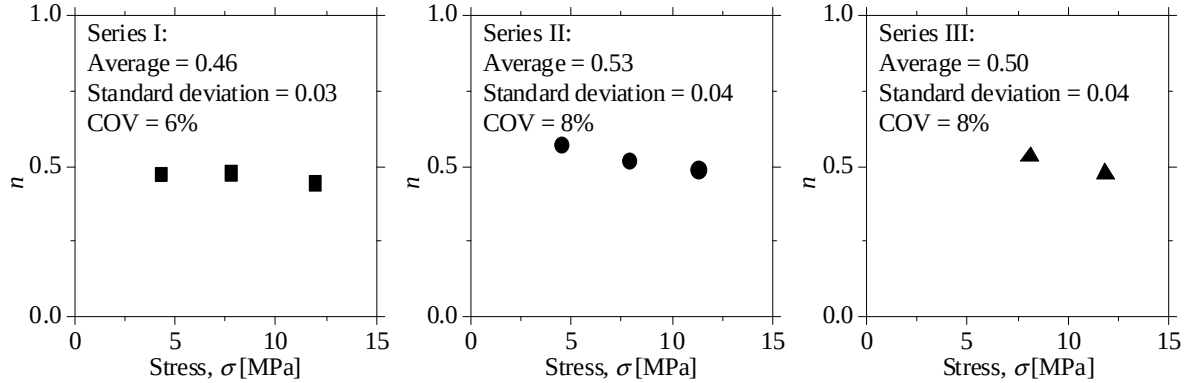

Figure 12: Parameter *n* vs. stress relationship.

3.4 Experimental creep curves

The main purpose of the tensile creep tests is to obtain the curves defining the tensile creep behaviour. One of those curves is known as the creep-modulus curve, defined in Eq. (4) and depicted afterwards in Figure 13.

$$E_{creep} = \frac{\sigma}{\varepsilon(t)} = \frac{1}{1/E_M + t/\eta_M + 1/E_K \left(1 - e^{-\left(\frac{E_K}{\eta_K} t\right)^{1-n}}\right)} \tag{4}$$

For the construction of this creep-modulus curve, the parameters reported in Table 4 were used. The values of the parameters were considered directly from the regressions and averages depicted from Figures 8 to 12.

Due to the consideration of constant parameters and, since the stress is by this process removed from the analysis as proven by Eq. (4), a constant creep-modulus curve is obtained for each series.

Table 4: Creep parameters.

Series	E_M [GPa]	η_M [GPa·h]	E_K [GPa]	η_K [GPa·h]	n
Series I	9.49	13482	5.27	129	0.46
Series II	8.80	11544	4.50	89	0.53
Series III	8.84	18446	3.09	58	0.50

Average, (Standard Deviation) and [Coefficient of variation]

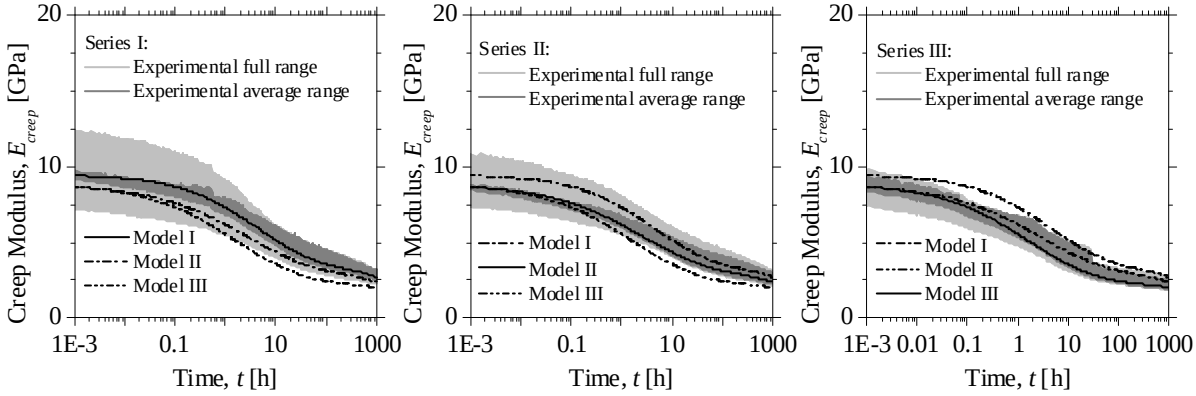

Figure 13: Creep modulus curves.

4. CONCLUSIONS

In this paper an experimental program aiming to assess the tensile creep behaviour of epoxy adhesives was presented. The analysis of the results obtained in these tests showed that the modified Burgers model is able of predicting with high accuracy the time dependent tensile strain of the material under study. Up to applied stress levels of 60% of the material's tensile strength, the instantaneous and time dependent properties of the tested adhesive were found to be constant under constant temperature and humidity Additional experimental tests should be performed not only to validate the results obtained, but also to determine the variation of the relevant parameters under different temperature/humidity.

ACKNOWLEDGMENTS

The study reported in this paper was supported by FCT, SFRH/BD/61756/2009, and is part of the project PreLami - Performance of reinforced concrete structures strengthened in flexural with an

innovative system using prestressed NSM CFRP laminates, with the reference PTDC/ECM/114945/2009. The authors would also like to acknowledge the support provided by S&P, for supplying the adhesives for the experimental program.

REFERENCES

[1] R.G. Wight, M.F. Green and M-A. Erki, "Prestressed FRP Sheets for Poststrengthening Reinforced Concrete Beams", Journal of Composites for Construction, Vol. 5, No. 4, 2011, pp. 214-220.
[2] H. Nordin, B. Täljsten, "Concrete Beams Strengthened with Prestressed Near Surface Mounted CFRP", Journal of Composites for Construction, Vol. 10, No. 1, 2006, pp. 60-68.
[3] M.A. Gaafar, R. El-Hacha, "Concrete Beams Strengthened with Prestressed Near Surface Mounted CFRP", International Conference on FRP Composites in Civil Engineering, 2008, 6 pp.
[4] R.A. Lopez-Anido, T.R. Naik, "Emerging Materials for Civil Engineering Infrastructure - State of the Art", ASCE Press, 2000.
[5] E.Y. Sayed-Ahmed, N.G. Shrive, "A new steel anchorage system for post-tensioning applications using carbon fibre reinforced plastic tendons." Canadian Journal of Civil Engineering, Vol. 25, No. 1, 1998, pp. 113-127.
[6] C. Li, K. Potter, M.R. Wisnom, G. Stringer, "In-situ measurement of chemical shrinkage of MY750 epoxy resin by a novel gravimetric method", Composites Science and Technology, Vol. 64, No. 1, 2004, pp. 55-64.
[7] H. Yu, S. Mhaisalkar, E. Wong, "Cure shrinkage measurement of nonconductive adhesives by means of a thermomechanical analyzer", Journal of Electronic Materials, Vol. 38, No. 4, 2005, pp. 1177-1182.
[8] C.W. Feng, C.W. Keong, Y.P. Hsueh, Y.Y. Wang, H.J. Sue, "Modeling of long-term creep behavior of structural epoxy adhesives", International Journal of Adhesion & Adhesives, Vol. 25, No. 5, 2005, pp. 427-436.
[9] ASTM 2990, "Standard Test Methods for Tensile, Compressive, and Flexural Creep and Creep-Rupture of Plastics" American Society for Testing and Materials, 2001.
[10] ISO 899-1, "Plastics - Determination of creep behaviour - Part 1: Tensile creep" International Organization for Standardization, 2003.
[11] H.F. Brinson, L.C. Brinson, "Polymer Engineering Science and Viscoelasticity: An Introduction." Springer Science & Business Media, 2008.
[12] ISO 527-2, "Plastics - Determination of tensile properties - Part 2: Test conditions for moulding and extrusion plastics" International Organization for Standardization, 1993.